JACS
JOURNAL OF THE AMERICAN CHEMICAL SOCIETY

Article

pubs.acs.org/JACS

Nucleation Effects in Peptide Foldamers

Anupam Patgiri,‡ Stephen T. Joy,‡ and Paramjit S. Arora*

Department of Chemistry, New York University, New York, New York 10003, United States

Supporting Information

ABSTRACT: Oligomers composed of β^3-amino acid residues and a mixture of α- and β^3-residues have emerged as proteolytically stable structural mimics of α-helices. An attractive feature of these oligomers is that they adopt defined conformations in short sequences. In this manuscript, we evaluate the impact of β^3-residues as compared to their α-amino acid analogs in prenucleated helices. Our hydrogen−deuterium exchange results suggest that heterogeneous sequences composed of "$\alpha\alpha\alpha\beta$" repeats are conformationally more rigid than the corresponding homogeneous α-peptide helices, with the macrocycle templating the helical conformation having a significant influence.

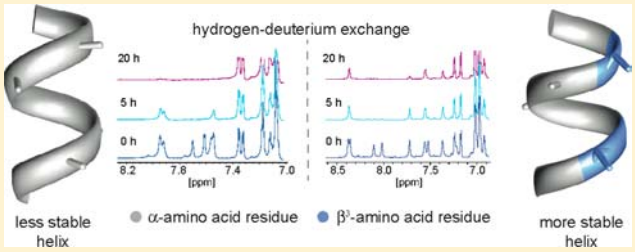

INTRODUCTION

Conformationally defined synthetic oligomers, termed foldamers, have emerged as attractive molecular scaffolds for the discovery of new materials, catalysts and ligands for protein receptors.[1−5] Oligomers composed of β^3- and mixtures of α- and β^3-residues represent well-studied classes of foldamers, specifically as mimics of α-helices and inhibitors of previously intractable protein−protein interactions.[6−12] One surprising aspect of β-peptide oligomers is that they assume defined helical structures in very short sequences despite the presence of the extra methylene units which would be expected to endow the backbone with an increased freedom of rotation.[2,6,13] In contrast, α-peptides composed of less than 15 α-amino acids generally do not adopt defined helical conformations, in the absence of structural constraints. The helix−coil theory suggests that long sequences and multiple intramolecular hydrogen bonds are needed in order to overcome the energetically demanding nucleation parameter.[14−18] Attainment of helical configurations in β-peptides composed of as little as six residues suggests that the nucleation or the propagation parameter is distinct in helices containing β^3-residues.[13] In this manuscript, we compare the helical propensities of α- and β^3-amino acids in prenucleated helices. Such comparisons have been challenging because the circular dichroism (CD) spectra of α-peptides and peptides containing β^3-residues feature different sets of maxima and minima.[9,19,20] Although a number of β-peptide foldamers have been crystallized, the contribution of crystal structure packing to the observed conformation is difficult to quantify. Our results suggest that oligomers composed of "$\alpha\alpha\alpha\beta$" repeats are more stable than their α-peptide analogs.[9,10,13] We also investigated the protein-binding properties of $\alpha3\beta$-oligomers and found that the heterogeneous oligomer can bind the target receptor with a similar affinity to the α-peptide. A combination of the biophysical and protein binding results provides valuable insights for designing $\alpha3\beta$ foldamers. Importantly, the results suggest that the underlying strategy provides a unique approach for comparing properties of nonnatural residues to known parameters of α-amino acids.

RESULTS AND DISCUSSION

We designed a host helix in which the propensity of α- and β^3-guest residues could be evaluated.[21−29] Helices were nucleated using the hydrogen-bond surrogate (HBS) approach, in which a N-terminal $i \rightarrow i + 4$ intramolecular hydrogen bond is replaced with a covalent bond (Figure 1a).[30] The HBS approach leads to defined α-helices in short peptides. Solution and solid-state conformations of HBS helices have previously been characterized with 2D NMR and CD spectroscopies and X-ray crystallography.[31,32] Comparisons of experimental thermal denaturation curves with simulations of the Zimm−Bragg model[14−17] suggest that HBS helices are nucleated with the constant, σ, close to unity.[32−35] We have also demonstrated that HBS α-helices can target their cognate protein receptors with high affinity and specificity.[36−40] Significantly, the stabilized α-helices can modulate chosen intracellular protein−protein interactions, while their unconstrained counterparts remain ineffective.[36,37]

The key advantage of the HBS approach is its ability to provide conformational rigidity in short peptides without utilizing side chain functionality. Oligomers composed of β^3- and mixtures of α- and β^3-residues are typically preorganized using cyclic amino acid analogs with predefined ϕ-, ψ-dihedral angles,[8,41,42] or through side chain to side chain contacts,[7,12,43−45] for example, where one side of the helix has a hydrophobic face and a second features ionic bridges. A drawback of the latter strategy is that it limits the diversity of side chains that may be placed on a helix for specific biomolecular recognition. An attractive feature of the HBS method is that it provides conformational control over sequences composed of acyclic residues without sacrificing side

Received: February 28, 2012
Published: June 20, 2012

   dx.doi.org/10.1021/ja301953j | J. Am. Chem. Soc. 2012, 134, 11495−11502

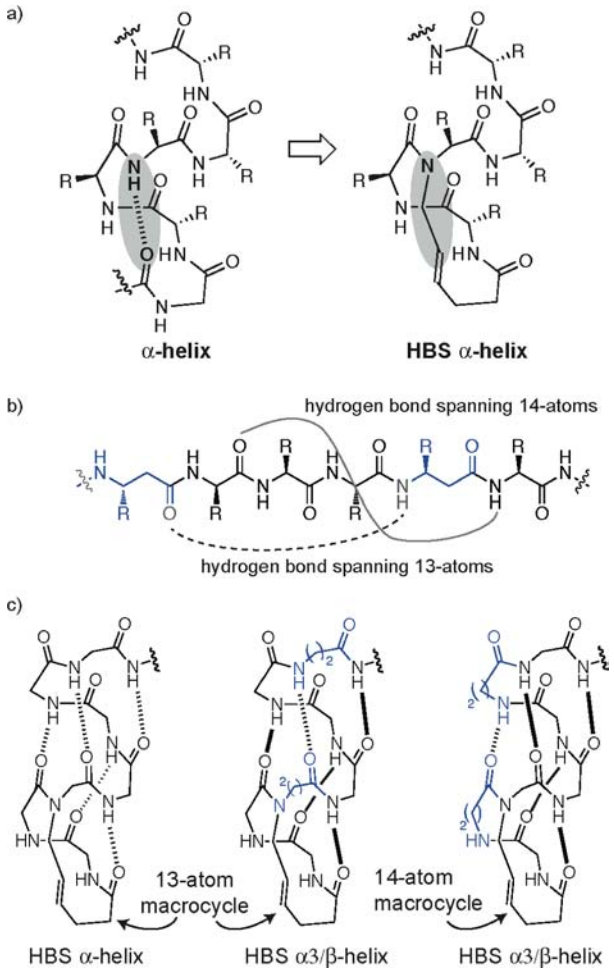

Figure 1. (a) HBS α-helices feature a carbon−carbon bond in place of an N-terminal main-chain (i, i + 4) hydrogen bond. (b) An $\alpha3\beta$-sequence contains 13- and 14-membered hydrogen bonds. (c) Design of HBS α- and HBS $\alpha3\beta$-peptides with different nucleation macrocycles; hydrogen bonds spanning 13 and 14 atoms are shown as hashed and bold bonds, respectively.

chain functionalities. Herein we show that conformationally defined chimeric helices can be accessed from acyclic residues with the HBS strategy.

Prenucleated HBS helices allow us to monitor the subtle effects of $\alpha \rightarrow \beta^3$ substitution on helix propagation while controlling the nucleation parameters. We inserted one β^3-residue per helical turn in the host HBS α-helix such that the heterogeneous sequence contains three α-residues followed by one β^3-residue. Such $\alpha3\beta$ sequences have previously been characterized as suitable mimics of α-helices.[9] We based the oligomer design on a short segment from the p53 activation domain,[46] whose design and protein binding properties have been previously reported (Table 1).[38,47] This sequence was chosen to allow us to investigate the potential of HBS $\alpha3\beta$-analogs to target murine double minute 2 (MDM2) in comparison to the parent HBS α-helix. The p53 sequence was also deemed appropriate because it lacks multiple side chain contacts, such as ionic bridges, which may bias the results. The parent constrained α-peptide is roughly 50% helical according to CD spectroscopy.[38,47] We conjectured that this range was ideal for examining potential increase or decrease in conformational rigidity of the heterogeneous oligomers.

Table 1. Design of α- and $\alpha3\beta$-Peptides

peptide	sequence[a]
HBS α-helix **1**	XQEG*FSDLWKLLS-NH_2
HBS $\alpha3\beta$-helix **2**	XQE**G**$_\beta$*FSD**L**$_\beta$WKL**L**$_\beta$S-NH_2
HBS $\alpha3\beta$-helix **3**	XQ**E**$_\beta$G*FS**D**$_\beta$LWKL$_\beta$LS-NH_2
$\alpha3\beta$-peptide **4**	AcQ**E**$_\beta$GFS**D**$_\beta$LWKL$_\beta$LS-NH_2

[a]X, G*, and G$_\beta$* denote 4-pentenoic acid, *N*-allyl glycine, and *N*-allyl β-alanine residues, respectively. Bold letters denote β^3-residues.

Design of the $\alpha3\beta$-helices raises an interesting question regarding the nucleation of heterogeneous sequences. A canonical $\alpha3\beta$ sequence would be expected to feature hydrogen bonds spanning 13 atoms within turns comprised of α-residues but 14-membered hydrogen bonds in turns that contain a β^3-residue (Figure 1b). This alternating pattern of putative hydrogen bonds within folded oligomers is unique to heterogeneous sequences, although 3(10) helices with 10-membered intramolecular hydrogen bonds are known to initiate α-helical regions within proteins.[48] We conjectured that the stability of the $\alpha3\beta$-sequences would fluctuate with the size of the nucleation macrocycle. A 13-membered HBS macrocycle is a mimic of a tripeptide α-helical turn and promotes intramolecular hydrogen bonds that span 13 atoms in canonical α-helices. HBS **1** is a mimic of an α-helix with a 13-membered HBS macrocycle. However, a 13-membered macrocycle would not be expected to be optimal if it is followed by a β^3-residue and 3 successive 14-atom intramolecular hydrogen bonds, as in HBS **2**. The 13- and 14-membered hydrogen bonds are shown as hashed and bold bonds, respectively, in Figure 1c. A 14-membered HBS macrocycle, as in HBS **3**, with an embedded β^3-residue should be a better nucleator of $\alpha3\beta$-sequences. In support of this hypothesis, we have previously shown that stability of α-helices is optimal with a 13-membered HBS macrocycle replacing the 13-membered intramolecular hydrogen bond rather than a 14-membered HBS macrocycle.[33]

Design and Synthesis. We began the design of HBS $\alpha3\beta$-helices by examining the potential of a 13- and a 14-membered macrocycle to control the desired helical conformation in the attached peptide (Figure 1c and Table 1). HBS helices contain a carbon−carbon bond in place of a main chain $i \rightarrow i + 4$ hydrogen bond. The hydrocarbon bridge is inserted using a ring-closing metathesis reaction between two appropriately placed alkene groups (Supporting Information).[49] Detailed protocols for the synthesis of the HBS helices have been reported previously.[50−53]

Structural Characterization by CD. The helicity of the peptides was examined by CD spectroscopy. CD studies were performed in 10% trifluoroethanol (TFE) in phosphate buffered saline (PBS). The organic cosolvent was included because the p53-derived sequence aggregates in pure aqueous solutions. In 10% TFE, molar ellipticity remained consistent between 25 and 120 μM concentration range, indicating reduced aggregation effects (Supporting Information, Figure S6). Figure 2a shows the CD spectra of **1**−**3**. HBS α-helix **1** affords a CD signature typical of a canonical α-helix, with double minima near 206 and 222 nm and a maximum at 190 nm.[38] The traces obtained for HBS $\alpha3\beta$ **2**−**3** are similar to those observed for α-helices except with a weaker 222 nm band. It is difficult to compare the conformational stability of these three different oligomers using CD since they all contain different structural topographies and feature different minima.[54] The unconstrained $\alpha3\beta$-peptide analog **4** provides weaker signal as compared to the constrained derivative consistent with the idea that conformational rigidity is endowed

dx.doi.org/10.1021/ja301953j | J. Am. Chem. Soc. 2012, 134, 11495−11502

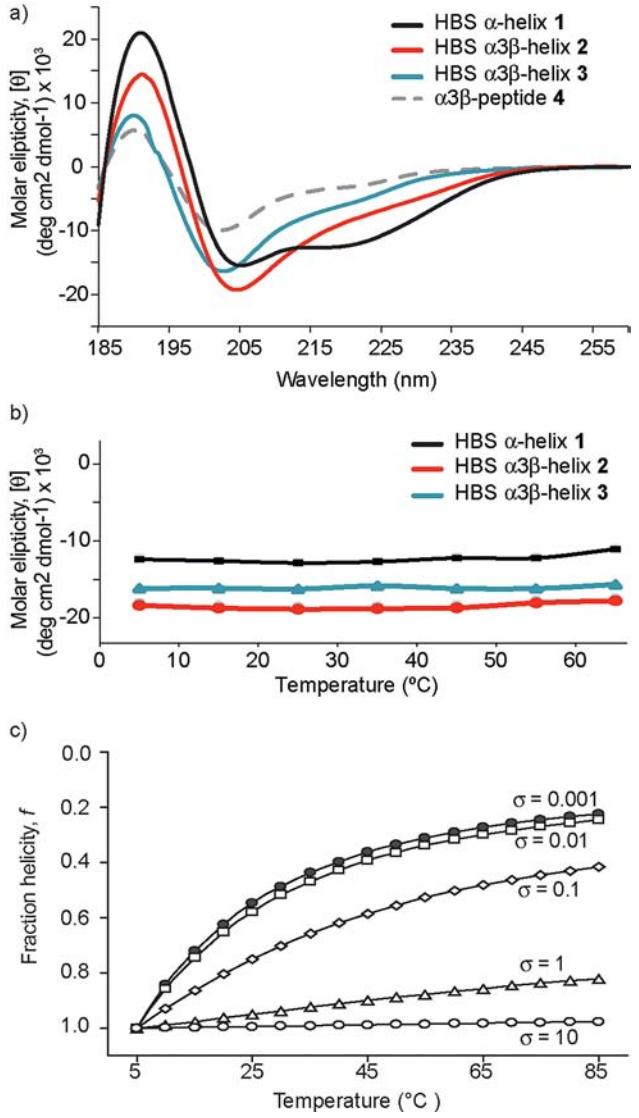

Figure 2. (a) CD spectra of peptides **1**−**4** at 25 °C. (b) Effect of temperature on the stability of HBS helices. The CD spectra were obtained in 10% TFE/PBS. Denaturation of **1**−**3** was monitored at 222, 205, and 202 nm wavelengths, respectively. (c) Theoretical denaturation curves as a function of different nucleation constant, σ. The theoretical curves were obtained by simulating the Zimm−Bragg model for a helix that can only denature in one direction, as described.[33]

by the HBS constraint (Figure 2a). The CD spectrum of the $\alpha 3\beta$-sequences are consistent with the previously reported spectrum of β- and chimeric α/β-peptides in shape and intensity.[20,55]

Thermal Stability of HBS Helices 1−3. We next investigated the thermal stability of HBS helices by monitoring the temperature-dependent change in its CD spectrum (Figure 2b). Previous thermal denaturation studies with HBS helices have shown that the conformation of these nucleated peptides stays remarkably consistent at high temperatures.[32−34] The broad melting transition in HBS helices is consistent with $\sigma \geq 1$.[56] This σ value (and the broad transition) implies a noncooperative case in which each unit behaves independently, as shown by the simulation of the Zimm−Bragg model for a helix that can only denature in one direction (Figure 2c).[14−17,33] The thermal denaturation curves show that both HBS $\alpha 3\beta$ **2** and **3** retain the broad melting characteristics of HBS helices with $\sigma \geq 1$ and highlight the potential of the HBS strategy to nucleate heterogeneous sequences composed of acyclic residues. The results also indicate that both the 13- and 14-membered macrocycles in **2** and **3** are capable of initiating defined conformations.

Structural Characterization by NMR. CD spectroscopy provides compelling evidence that the hydrogen-bond surrogate approach can stabilize heterogeneous sequences. However, CD spectroscopy does not allow a detailed analysis of the peptide structure at the atomic level. For instance, we wanted to determine if individual β^3-residues propagate with similar effectiveness as the α-residues. For answers to these pertinent questions, we fully characterized the compounds by NMR spectroscopy. The NMR studies were performed in 20% CF_3CD_2OD in PBS (pH 3.5) rather than in lower amounts of TFE-d_3; we used this solvent mixture for two reasons: (1) In purely aqueous solutions or 10% TFE solutions, these sequences showed observable aggregation at concentrations needed for NMR studies, while aggregation effects were negligible in 20% TFE, and (2) this solvent system provided minimal peak overlap, allowing unambiguous assignment of a larger number of resonances. To evaluate the conformational stability and dynamics of **1**−**3**, we obtained rates of amide proton H/D exchange, which provide a convincing measure of the extent to which a particular main chain proton is involved in intramolecular hydrogen bonding.[57,58]

We utilized a combination of 1D and 2D NMR experiments to further define the conformation of **1**−**3**. A set of 2D total correlation (TOCSY) and nuclear Overhauser enhancement (NOESY) spectroscopies were used to assign ^{1}H NMR resonances for **1**−**3**. Sequential NH−NH (i and i + 1) NOESY cross-peaks, a signature of helical structure, were observed for **1**−**3** as shown in the NOE correlation charts (Figure 3 and Supporting Information). The NOESY spectra further reveal several medium to weak (i, i + 3) and (i, i + 4) NH−CHα cross peaks that support an α-helix-like conformation in these peptides. A larger number of contiguous medium range NOEs, suggestive of a more stable helical conformation, are seen with **3** than the other two peptides. Analysis suggests predominance of a single helical conformation in both HBS $\alpha 3\beta$-sequences. This result is important because earlier solution studies have indicated a mixture of two conformations is observed in oligomers composed of acyclic β^3-residues.[59,60]

Amide H/D Exchange Rates. Main-chain amide hydrogen−deuterium exchange rates offer a sensitive measure of structural stability and dynamics of proteins.[57,61,62] Structured protein amide protons are involved in backbone hydrogen bonding and are shielded from solvents resulting in their slow H/D exchange kinetics compared to unstructured protein amide protons. Figure 4 shows spectra for **1**−**3** at different time intervals following the addition of D_2O. The tabulated exchange values for residues outside the HBS macrocycle for oligomers **1**−**3** are shown in Tables 2−4. The individual hydrogen-exchange rates in these helices can be determined precisely which is typically not possible for short peptides, indicating the conformational stability of these oligomers. The measured exchange rates, k_{ex}, were compared to the predicted intrinsic chemical exchange rate, k_{ch}, for an unstructured α-peptide of the same sequence, to assess individual protection factors ($\log k_{ch}/k_{ex}$) and the corresponding free energies of protection ($-\Delta G$).[63] The predicted intrinsic chemical exchange rates, protection factors, and the free energy of protection were calculated using the spreadsheet at http://hx2.med.upenn.edu and are shown in Table 2. (This worksheet

dx.doi.org/10.1021/ja301953j | J. Am. Chem. Soc. 2012, 134, 11495−11502

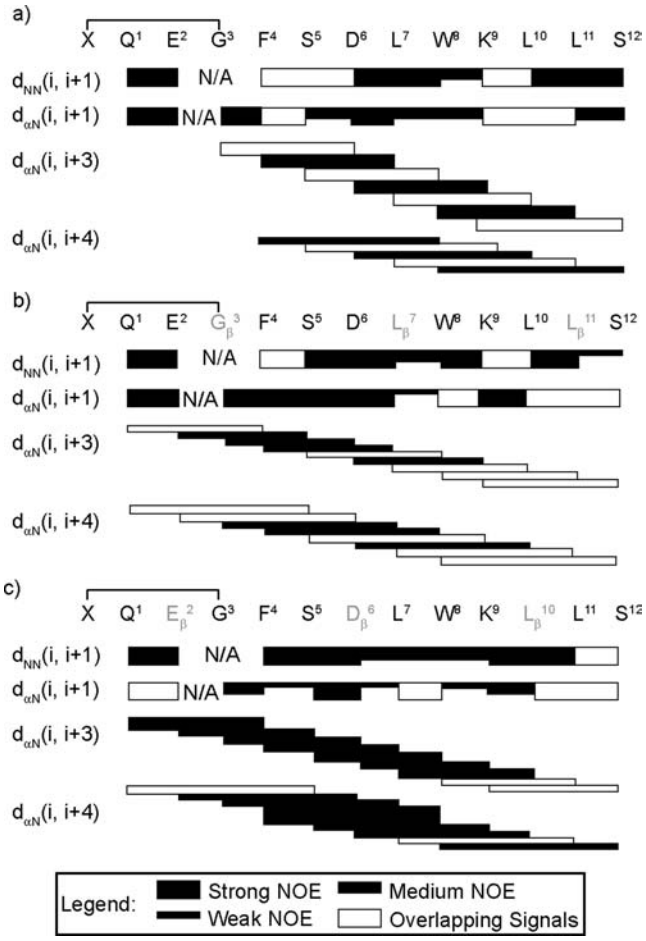

Figure 3. (a–c) NOESY correlation charts for **1**–**3**, respectively. The NMR spectra, included in the Supporting Information, were obtained in 20% TFE/PBS. Gray letters denote β^3-residues, while α refers to CH protons adjacent to the amide NH in α- and β^3-amino acid residues.

was developed for α-peptides and not for heterogeneous sequences; however, we think its use offers critical insights.)

The H/D spectra suggest a striking degree of stability in **3**; more of the amides remain partially protected after 10 h in **3** than **1** and **2**. Nearly all NH protons have exchanged after 20 h of incubation in **1** and **2**, but some residues retain their proton label in **3** even after 24 h. Several residues in **3** are protected from exchange with free energy values of 1 kcal/mol or greater than in **1** and **2**. Overall, the data indicate that peptide **3** with the HBS macrocycle of 14-atoms templating two successive 14-atom hydrogen bonds is more stable than peptide **2** with a 13-membered macrocycle nucleating three consecutive 14-atom hydrogen bonds (Figure 1c). This result is in line with our previous observation that α-helices containing a 13-membered HBS macrocycle are more conformationally stable than those containing an extra atom in the template.[33] Significantly, the exchange rates in oligomer **3** are much slower than in **1** suggesting that β^3-residues have a higher helical propensity than α-residues. The $\alpha3\beta$-peptide **3** contains a highly stable hydrogen-bonded network with significant protection factors and associated free energies of protection. Such a degree of stabilization is typically observed for buried amide protons in proteins but not in short peptides.[32,58] H/D exchange rates of oligomers **1** and **2**, both of which contain 13-membered nucleation cycles, are similar in magnitude. This interesting result highlights the conflicting factors contributing to conformational stability of **2** and supports results seen with **3**; the nucleation in **2** is not optimal, however, the higher helical propensity of β^3-residues stabilizes the conformation. Comparison of exchange rates for F4 and S5, the two residues that follow the macrocycle, in the three sequences is particularly revealing: These amides in **3** exchange much more slowly than in **1** and **2** indicating that the 14-membered macrocycle endows a high level of conformational rigidity. This result has significant implications for the future design of HBS helices as inhibitors of biomolecular interactions.

Solution Structure of 3. The solution structure of the HBS **3** was determined from NOESY cross-peaks and $^3J_{NHC\alpha H}$ coupling constants (Supporting Information, Table S6) using Monte Carlo conformational search in Macromodel 2011.[64,65] A total of 200 NOE restraints (45 medium and long-range, 51 sequential, and 104 intraresidue) and 11 ϕ angle restraints were used during the dynamics. No explicit hydrogen-bond restraints were used in the calculations. The final 20 lowest energy structures had no significant distance violations (Figure 5). The 20 conformer ensemble obtained for the peptide shows a backbone root mean squared deviation (rmsd) of 0.47 ± 0.06 Å. From the top down view, it can be seen that the macrocycle does not protrude from the helix (Figure 5b). Overall, the NMR structure of **3** confirms that a well-defined conformation is accessed in this $\alpha3\beta$-helix.

Potential to Target Protein Receptors that Recognize α-Helices. The CD and NMR studies provide compelling evidence that HBS $\alpha3\beta$-helices **2** and **3** adopt configurations similar to that of an α-helix. To evaluate the potential of HBS $\alpha3\beta$-helices to target proteins that recognize α-helices, we measured the affinity of **2**–**3** for MDM2. We performed fluorescence polarization-based competition binding experiments and found that **3** binds to MDM2 with high affinity (K_D = 80 ± 21 nM) comparable to that previously reported for the optimized HBS p53 α-helix analog **1** (Figure 5 and Supporting Information).[38] Surprisingly, HBS $\alpha3\beta$-helix **2** targets MDM2 (K_D = 12.6 ± 1.8 μM) with a 150-fold lower affinity than **3**. This large change may be attributed to two factors: (1) the differential conformational stability between peptides **2** and **3**, and (2) the precise placement of the β-residues between peptide **2** and **3**. In **3**, all three of the p53 residues (Phe19, Trp23, and Leu26 in protein data bank numbering), which make important contacts with MDM2, are retained as α-amino acids;[46] whereas in **2**, Leu11 or Leu26 in PDB numbering, has been converted to the β-analog. It is unclear if minor distortions caused by β-Leu may be leading to decreased affinity.[9]

The high affinity of **3** for MDM2 demonstrates that judicious substitution of α-residues with β^3-residues in HBS helices does not introduce structural perturbations that compromise their binding. To evaluate the specificity of HBS **3** for MDM2, we designed a negative control (HBS **5:** XQEβG*ASD$_\beta$LWKL$_\beta$AS-NH_2) by mutating two of the residues important for binding in **3** (Phe 19 and Leu 26) to alanines. As expected, compound **5** does not bind to MDM2 with measurable affinity (Figure 6). MDM2 has previously been targeted with β-peptide oligomers.[11,66–71] $\alpha3\beta$-**3** competes favorably with these oligomers with regards to its K_D for MDM2. Studies to evaluate the potential of this p53 mimetic to reactivate the p53 pathway are underway.[72]

■ CONCLUSIONS

The studies described herein were designed to investigate three broad questions pertaining to the design of nonnatural peptide oligomers: (1) Can the HBS nucleation strategy effectively

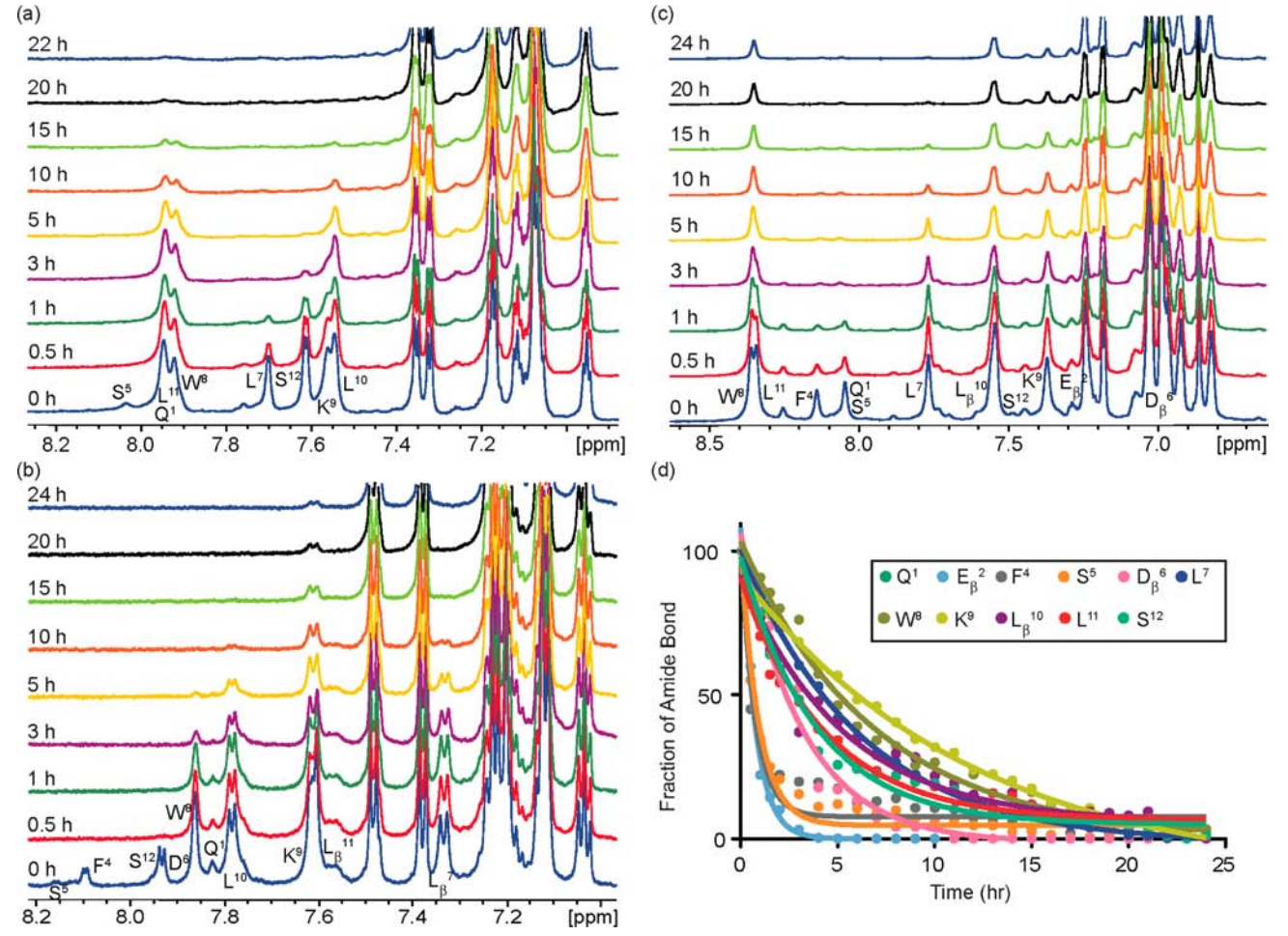

Figure 4. (a–c) H/D exchange spectra for backbone amide protons in **1**–**3**, respectively. (d) Exchange curves for **3**. The H/D exchange experiments were performed in duplicate. The NMR spectra were obtained in 20% TFE/PBS.

Table 2. Summary of Amide Proton Temperature Coefficients and Deuterium Exchange Data for 1

peptide **1** residues	F^4	S^5	D^6	L^7	W^8	K^9	L^{10}	L^{11}	S^{12}
H/D rate constant × 10^{-5} (h^{-1})	38.08	38.08	38.08	1.69	0.18	0.51	0.20	0.17	0.78
protection factor (log k_{ch}/k_{ex})[a]	−0.81	−0.32	0.14	0.54	0.96	0.97	1.08	0.84	1.09
stabilization, −ΔG (kcal/mol)	N/A	N/A	−0.58	0.52	1.22	1.23	1.40	1.04	1.42

[a]Calculated using the spreadsheet at http://hx2.med.upenn.edu download.html. k_{ex}: measured exchange rates, and k_{ch}: intrinsic chemical exchange rate.

Table 3. Summary of Amide Proton Temperature Coefficients and Deuterium Exchange Data for 2[a]

peptide **2** residues	F^4	S^5	D^6	$\mathbf{L}_{\beta}^{7}$	W^8	K^9	L^{10}	$\mathbf{L}_{\beta}^{11}$	S^{12}
H/D rate constant × 10^{-5} (h^{-1})	38.09	38.09	4.17	0.20	0.69	0.28	0.32	0.25	5.85
protection factor (log k_{ch}/k_{ex})	−0.59	−0.10	1.32	1.70	0.61	1.45	1.07	0.89	0.44
stabilization, −ΔG (kcal/mol)	N/A	N/A	1.76	2.30	0.66	1.95	1.40	1.12	0.33

[a]β^3-residues are shown in bold font.

Table 4. Summary of Amide Proton Temperature Coefficients and Deuterium Exchange Data for 3[a]

peptide **3** residues:	F^4	S^5	$\mathbf{D}_{\beta}^{6}$	L^7	W^8	K^9	$\mathbf{L}_{\beta}^{10}$	L^{11}	S^{12}
H/D rate constant × 10^{-5} (h^{-1})	1.33	1.07	0.32	0.16	0.14	0.08	0.19	0.23	0.26
protection factor (log k_{ch}/k_{ex})	0.65	1.23	2.22	1.56	1.07	1.75	1.1	0.70	1.58
stabilization, −ΔG (kcal/mol)	0.72	1.61	2.97	2.07	1.39	2.34	1.43	0.8	2.10

[a]β^3-residues are shown in bold font.

stabilize heterogeneous sequences composed of α- and β^3-residues?; (2) Since $\alpha3\beta$-oligomers may contain 13 or 14 atom

dx.doi.org/10.1021/ja301953j | J. Am. Chem. Soc. 2012, 134, 11495–11502

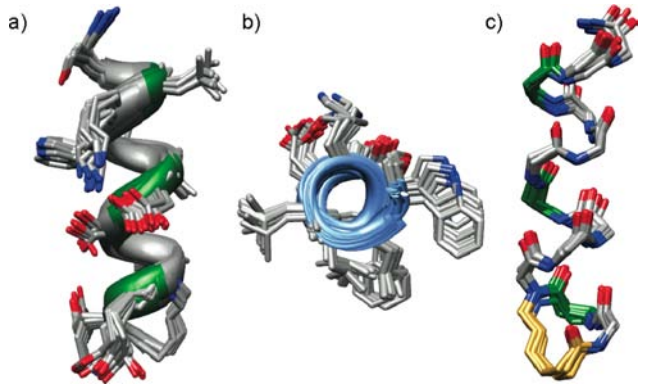

Figure 5. NMR-derived structures of HBS $\alpha 3\beta$-helix **3**. Side (a,c) and top (b) views of 20 lowest energy structures. Carbon, nitrogen, and oxygen atoms are shown in gray, blue, and red, respectively, except in (c) where the hydrocarbon bridge is shown in gold color. The β-residues are highlighted in green.

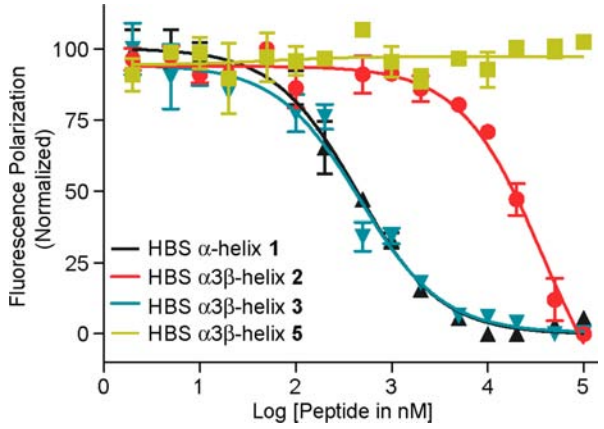

Figure 6. Determination of peptide binding to His_6-tagged MDM2 by a fluorescence polarization assay.

intramolecular hydrogen bonds, which size nucleus would best stabilize the resulting foldamers?; and (3) in optimally prenucleated systems, are $\alpha 3\beta$- or all α-sequences more stable?

This study shows that the HBS method compares favorably with previous approaches in stabilizing oligomers composed of α- and β^3-residues.[8,12,41−45] The results also illustrate that the optimum $\alpha 3\beta$-oligomer **3** is more conformationally defined than HBS α-helix **1**, in line with the stable β conformations observed in crystal and NMR structures.[6,9,13,73,74] Importantly, the studies provide a host scaffold for evaluating the propensities of β-amino acids. The Cα−Cβ torsion angles of the β-residues in the calculated lowest energy NMR structure of **3** (Figure 5) are 64.6° and 56.9° in D6 and L10, respectively. These values suggest that the preferred angle of 60° for the Cα−Cβ torsion in homogeneous 3_{14}-helices may be accessible in $\alpha 3\beta$-helices,[74,75] although in $\alpha 3\beta$ crystal structures this angle is found to range between 70 and 80°.[9,13,76]

Oligomer **3** with a 14-membered HBS macrocycle provides a highly stable $\alpha 3\beta$-foldamer as compared to the 13-membered macrocycle in **2**. This result speaks to the effective volume and helical pitch of α- versus β^3-residues. Crystal structure overlays by Gellman et al. suggest that $\alpha\alpha\beta\alpha\alpha\beta$ and $\alpha 3\beta$ repeats are suitable mimics of α-helices.[9,10] If the β^3-residues have a similar pitch as the α-residues in these scaffolds, a 13- versus 14-atom nucleus should stabilize the foldamer to a similar extent. The CD results indicate that the two oligomers are equally stable, supporting the solid-state structures;[9] however, subtle differences emerge in the NMR H/D exchange data. Although we designed the study with a biological sequence to obtain binding information, it was carefully chosen to avoid any apparent sequence-dependent effects biasing the results. We are currently examining other biological sequences to confirm the finding that conformational stability of nucleated α-helices can be significantly enhanced by judicious incorporation of β^3-residues. Combined, the analyses illustrate the potential of prenucleated helices to evaluate fundamental properties of nonnatural residues while controlling for any differences in nucleation.[35] In ongoing studies we are using the lessons learned in the present work to design next generations of protein−protein interaction inhibitors.

EXPERIMENTAL SECTION

General. Commercial-grade reagents and solvents were used without further purification except as indicated. Dichloroethane was distilled before use in the metathesis reactions. All reactions were stirred magnetically or mechanically shaken; moisture-sensitive reactions were performed under nitrogen or argon atmosphere. Reverse-phase HPLC experiments were conducted with 0.1% aqueous trifluoroacetic acid and 0.1% trifluoroacetic acid in acetonitrile buffers as eluents on C_{18} reversed-phase columns using a Beckman Coulter HPLC equipped with a System Gold 168 Diode array detector. ESI-MS data were obtained on an Agilent 1100 series LC/MSD (XCT) electrospray trap. The microwave reactions were performed in the CEM Discover single-mode reactor with controlled power, temperature, and time settings. Proton NMR spectra of HBS peptides were recorded on a Bruker AVANCE 600 or 900 MHz spectrometer.

Peptide Synthesis. Peptides were synthesized on a CEM Liberty microwave peptide synthesizer using Fmoc solid-phase chemistry on Rink amide resin and purified by reversed-phase HPLC.[52] The identity and the purity of the peptides were confirmed by ESI-MS.

Synthesis of HBS Helices. HBS **1**−**3** and HBS **5** were synthesized as previously described.[50−53] Briefly, peptide sequences up to the $i + 5^{th}$ residue of the putative helix were synthesized using Fmoc solid-phase chemistry on Rink amide resin on a CEM Liberty Series microwave peptide synthesizer. N-allylation of the $i + 4^{th}$ residue was achieved over two steps by coupling of bromoacetic acid followed by an allylamine displacement reaction (Supporting Information, Figure S1). Coupling of the next two Fmoc amino acid residues, followed by coupling of 4-pentenoic acid afforded the bis-olefin peptide.[52] Ring-closing metathesis of the bis-olefin peptide was performed with Hoveyda-Grubbs II catalyst in dichloroethane under microwave irradiation as described.[50,52] Metathesized peptides were cleaved from the resin using TFA/TIS/water (95:2.5:2.5), purified by reversed-phase HPLC (C_{18} column) and characterized by ESI-MS.

CD Spectroscopy. CD spectra were recorded on AVIV 202SF CD spectrometer equipped with a temperature controller using 1 mm length cells and a scan speed of 0.5 nm/min. The spectra were averaged over 10 scans with the baseline subtracted from analogous conditions as that for the samples. The samples were prepared in 0.1× phosphate buffered saline (13.7 mM NaCl, 1 mM phosphate, 0.27 mM KCl, pH 7.4), containing 10% trifluoroethanol, with the final peptide concentration of 100 μM. The concentrations of peptides were determined by the UV absorption of tryptophan residue at 280 nm. The helix content of the α-peptide was determined from the mean residue CD at 222 nm, $[\theta]_{222}$ (deg cm^2 dmol^{-1}) corrected for the number of amino acids. Percent helicity was calculated from the ratio $[\theta]222/[\theta]$max, where $[\theta]$max = $(-44\,000 + 250T)(1 - k/n)$, with $k = 4.0$ and n = number of residues.[32]

NMR Spectroscopy. Experiments were performed on a Bruker AVANCE 500, 600 or 900 MHz spectrometer equipped with a TXI probe (500 and 600) or a cryoprobe (900) and 3D gradient control. Samples were prepared by dissolving 2 mg of peptide in 450 μL of PBS buffer (137 mM NaCl, 10 mM phosphate, 2.7 mM KCl, pH 7.4) and 120 μL of TFE-d_3. The 1D proton spectra or 2D TOCSY spectra (when overlapping is severe) were employed to discern the chemical shifts of

dx.doi.org/10.1021/ja301953j | J. Am. Chem. Soc. 2012, 134, 11495−11502

the amide protons. Solvent suppression was achieved with a 3919 Watergate pulse sequence. All 2D spectra were recorded at 20 °C by collecting 4092 complex data points in the t_2 domain by averaging 64 scans and 128 increments in the t_1 domain with the States-TPPI mode. All TOCSY experiments are performed with a mixing time of 80 ms and NOESY with the mixing time of 200 ms. The data were processed and analyzed using the Bruker TOPSPIN program. The original free induction decays (FIDs) were zero-filled to give a final matrix of 2048 by 2048 real data points. A 90° $\sin^2$ window function was applied in both dimensions.

Amide Hydrogen−Deuterium Exchange Experiments. Lyophilized samples of **1**−**3** from the above experiments were dissolved in 300 μL of a D_2O/TFE-d_3 mixture (80/20) to initiate the H/D exchange. The pH of the solution was confirmed. Spectra were recorded on a preshimmed Bruker AVANCE 600 or 900 MHz spectrometer. The recorded temperature was 20 °C both inside and outside the probe. The dead time was ca. 2 min. The intensity changes for each amide proton was determined by monitoring either the HN peaks on 1D spectra or the cross-peaks between HN and HR on 2D TOCSY spectra when overlapping was severe. The peak height data were fit into one phase exponential equation to get the exchange rate constants using GraphPad Prism 4.0 program.

Structure Calculations. The solution structure of the peptide was computed using Monte Carlo conformational search in Macromodel 2011.[64,65] The macromodel force field was applied to a random starting conformation. A total of 74 conformers were obtained using 45 medium- and long-range, 51 sequential, and 104 intraresidue constraints. The 20 lowest energy structures from different starting conformations show minimal overall deviation. The NOE restraints were categorized into three groups: strong (2.5 Å upper limit), medium (4.0 Å upper limit), and weak (5.5 Å upper limit) (Supporting Information, Table S5). The $^3J_{NHCH\alpha}$ coupling constants for all residues except G3 (due to lack of amide hydrogen) were used to calculate ϕ angles by application of the Pardi parametrized Karplus equation.[77,78]

Description of Protein Binding Studies. The relative affinities of peptides for N-terminal His_6-tagged MDM2 (25−117) were determined using fluorescence polarization based competitive binding assay with fluorescein-labeled p53 peptide, **Flu-p53**. The polarization experiments were performed with a DTX 880 Multimode Detector (Beckman) at 25 °C, with excitation and emission wavelengths at 485 and 535 nm, respectively. All samples were prepared in 96 well plates in 0.1% pluronic F-68 (Sigma). Prior to the competition experiments, the affinity of the **Flu-p53** for MDM2 was determined by monitoring polarization of the fluorescent probe upon binding MDM2 (Supporting Information, Figure S4). For competition binding experiments, appropriate concentrations of the peptides (1 nM−100 μM) were added to the MDM2-Flu-p53 mixture, and the resulting solution was incubated at 25 °C for 1 h before measuring the degree of dissociation of Flu-p53 by polarization. The binding affinity (K_D) values reported for each peptide are the averages of 3−5 individual experiments and were determined by fitting the experimental data to a sigmoidal dose−response nonlinear regression model on GraphPad Prism 4.0.[79]

■ ASSOCIATED CONTENT

Ⓢ Supporting Information

Detailed descriptions of synthesis and characterization including NMR spectra and analytical HPLC traces. This material is available free of charge via the Internet at http://pubs.acs.org.

■ AUTHOR INFORMATION

Corresponding Author

arora@nyu.edu

Author Contributions

‡These authors contributed equally.

Notes

The authors declare no competing financial interest.

■ ACKNOWLEDGMENTS

We thank Neville Kallenbach for helpful discussions and Neal Zondlo (University of Delaware) for the His_6-MDM2 construct. This work was financially supported by the National Institutes of Health (GM073943). A.P. thanks the New York University for a Sokol Predoctoral Fellowship. Support from the National Science Foundation (CHE-0958457) in the form of an instrumentation grant is gratefully acknowledged. The 900 MHz NMR data were collected at the New York Structural Biology Center, a Strategically Targeted Academic Research (STAR) center supported by the New York State Office of Science, Technology and Academic Research.

■ REFERENCES

(1) Gellman, S. H. *Acc. Chem. Res.* **1998**, *31*, 173.
(2) Goodman, C. M.; Choi, S.; Shandler, S.; DeGrado, W. F. *Nat. Chem. Biol.* **2007**, *3*, 252.
(3) Hill, D. J.; Mio, M. J.; Prince, R. B.; Hughes, T. S.; Moore, J. S. *Chem. Rev.* **2001**, *101*, 3893.
(4) Huc, I. *Eur. J. Org. Chem.* **2004**, 17.
(5) Stigers, K. D.; Soth, M. J.; Nowick, J. S. *Curr. Opin. Chem. Biol.* **1999**, *3*, 714.
(6) Cheng, R. P.; Gellman, S. H.; DeGrado, W. F. *Chem. Rev.* **2001**, *101*, 3219.
(7) Seebach, D.; Gardiner, J. *Acc. Chem. Res.* **2008**, *41*, 1366.
(8) Horne, W. S.; Gellman, S. H. *Acc. Chem. Res.* **2008**, *41*, 1399.
(9) Boersma, M. D.; Haase, H. S.; Peterson-Kaufman, K. J.; Lee, E. F.; Clarke, O. B.; Colman, P. M.; Smith, B. J.; Horne, W. S.; Fairlie, W. D.; Gellman, S. H. *J. Am. Chem. Soc.* **2012**, *134*, 315.
(10) Horne, W. S.; Johnson, L. M.; Ketas, T. J.; Klasse, P. J.; Lu, M.; Moore, J. P.; Gellman, S. H. *Proc. Natl. Acad. Sci. U.S.A.* **2009**, *106*, 14751.
(11) Bautista, A. D.; Appelbaum, J. S.; Craig, C. J.; Michel, J.; Schepartz, A. *J. Am. Chem. Soc.* **2010**, *132*, 2904.
(12) Hart, S. A.; Bahadoor, A. B.; Matthews, E. E.; Qiu, X. J.; Schepartz, A. *J. Am. Chem. Soc.* **2003**, *125*, 4022.
(13) Seebach, D.; Matthews, J. L. *Chem. Commun.* **1997**, 2015.
(14) Zimm, B. H.; Bragg, J. K. *J. Chem. Phys.* **1959**, *31*, 526.
(15) Lifson, S.; Roig, A. *J. Chem. Phys.* **1961**, *34*, 1963.
(16) Matheson, R. R.; Scheraga, H. A. *Macromolecules* **1983**, *16*, 1037.
(17) Qian, H.; Schellman, J. A. *J. Phys. Chem.* **1992**, *96*, 3987.
(18) Yang, J. X.; Zhao, K.; Gong, Y. X.; Vologodskii, A.; Kallenbach, N. R. *J. Am. Chem. Soc.* **1998**, *120*, 10646.
(19) Price, J. L.; Hadley, E. B.; Steinkruger, J. D.; Gellman, S. H. *Angew. Chem., Int. Ed.* **2010**, *49*, 368.
(20) Price, J. L.; Horne, W. S.; Gellman, S. H. *J. Am. Chem. Soc.* **2010**, *132*, 12378.
(21) Horovitz, A.; Matthews, J. M.; Fersht, A. R. *J. Mol. Biol.* **1992**, *227*, 560.
(22) Rohl, C. A.; Chakrabartty, A.; Baldwin, R. L. *Protein Sci.* **1996**, *5*, 2623.
(23) Chakrabartty, A.; Baldwin, R. L. In *Advances in Protein Chemistry*; Anfinsen, C.B.; , Richards, F. M., Edsall, J. T., David, S. E., Eds.; Academic Press: Waltham, MA, 1995; Vol. *46*, p 141.
(24) Yang, J. X.; Spek, E. J.; Gong, Y. X.; Zhou, H. X.; Kallenbach, N. R. *Protein Sci.* **1997**, *6*, 1264.
(25) Munoz, V.; Serrano, L. *J. Mol. Biol.* **1995**, *245*, 275.
(26) O'Neil, K. T.; DeGrado, W. F. *Science* **1990**, *250*, 646.
(27) Kallenbach, N. R.; Lyu, P. C.; Zhou, H. X. In *Circular Dichroism and the Conformational Analysis of Biomolecules*; Fasman, G. D., Ed.; Plenum Press: New York, 1996.
(28) Blaber, M.; Zhang, X. J.; Lindstrom, J. D.; Pepiot, S. D.; Baase, W. A.; Matthews, B. W. *J. Mol. Biol.* **1994**, *235*, 600.
(29) Wojcik, J.; Altmann, K. H.; Scheraga, H. A. *Biopolymers* **1990**, *30*, 121.
(30) Patgiri, A.; Jochim, A. L.; Arora, P. S. *Acc. Chem. Res.* **2008**, *41*, 1289.

(31) Liu, J.; Wang, D.; Zheng, Q.; Lu, M.; Arora, P. S. *J. Am. Chem. Soc.* **2008**, *130*, 4334.
(32) Wang, D.; Chen, K.; Kulp, J. L.; Arora, P. S. *J. Am. Chem. Soc.* **2006**, *128*, 9248.
(33) Wang, D.; Chen, K.; Dimartino, G.; Arora, P. S. *Org. Biomol. Chem.* **2006**, *4*, 4074.
(34) Chapman, R. N.; Dimartino, G.; Arora, P. S. *J. Am. Chem. Soc.* **2004**, *126*, 12252.
(35) Chapman, R.; Kulp, J. L., III; Patgiri, A.; Kallenbach, N. R.; Bracken, C.; Arora, P. S. *Biochemistry* **2008**, *47*, 4189.
(36) Patgiri, A.; Yadav, K. K.; Arora, P. S.; Bar-Sagi, D. *Nat. Chem. Biol.* **2011**, *7*, 585.
(37) Henchey, L. K.; Kushal, S.; Dubey, R.; Chapman, R. N.; Olenyuk, B. Z.; Arora, P. S. *J. Am. Chem. Soc.* **2010**, *132*, 941.
(38) Henchey, L. K.; Porter, J. R.; Ghosh, I.; Arora, P. S. *ChemBioChem* **2010**, *11*, 2104.
(39) Wang, D.; Lu, M.; Arora, P. S. *Angew. Chem., Int. Ed.* **2008**, *47*, 1879.
(40) Wang, D.; Liao, W.; Arora, P. S. *Angew. Chem., Int. Ed.* **2005**, *44*, 6525.
(41) Appella, D. H.; Christianson, L. A.; Klein, D. A.; Powell, D. R.; Huang, X. L.; Barchi, J. J.; Gellman, S. H. *Nature* **1997**, *387*, 381.
(42) Vaz, E.; Pomerantz, W. C.; Geyer, M.; Gellman, S. H.; Brunsveld, L. *ChemBiochem* **2008**, *9*, 2254.
(43) Arvidsson, P. I.; Rueping, M.; Seebach, D. *Chem. Commun.* **2001**, 649.
(44) Kritzer, J. A.; Tirado-Rives, J.; Hart, S. A.; Lear, J. D.; Jorgensen, W. L.; Schepartz, A. *J. Am. Chem. Soc.* **2005**, *127*, 167.
(45) Cheng, R. P.; DeGrado, W. F. *J. Am. Chem. Soc.* **2001**, *123*, 5162.
(46) Kussie, P. H.; Gorina, S.; Marechal, V.; Elenbaas, B.; Moreau, J.; Levine, A. J.; Pavletich, N. P. *Science* **1996**, *274*, 948.
(47) Mahon, A. B.; Arora, P. S. *Chem. Commun.* **2012**, *48*, 1416.
(48) Bolin, K. A.; Millhauser, G. L. *Acc. Chem. Res.* **1999**, *32*, 1027.
(49) Grubbs, R. H. *Angew. Chem., Int. Ed.* **2006**, *45*, 3760.
(50) Chapman, R. N.; Arora, P. S. *Org. Lett.* **2006**, *8*, 5825.
(51) Dimartino, G.; Wang, D.; Chapman, R. N.; Arora, P. S. *Org. Lett.* **2005**, *7*, 2389.
(52) Patgiri, A.; Menzenski, M. Z.; Mahon, A. B.; Arora, P. S. *Nat. Protoc.* **2010**, *5*, 1857.
(53) Patgiri, A.; Witten, M. R.; Arora, P. S. *Org. Biomol. Chem.* **2010**, *8*, 1773.
(54) Driver, R. W.; Hoang, H. N.; Abbenante, G.; Fairlie, D. P. *Org. Lett.* **2009**, *11*, 3092.
(55) Sawada, T.; Gellman, S. H. *J. Am. Chem. Soc.* **2011**, *133*, 7336.
(56) Cantor, C. R.; Schimmel, P. R. *The behavior of biological macromolecules*; W. H. Freeman: San Francisco, CA, 1980, Chapter 20.
(57) Englander, S. W.; Kallenbach, N. R. *Q. Rev. Biophys.* **1983**, *16*, 521.
(58) Zhou, H. X. X.; Hull, L. A.; Kallenbach, N. R.; Mayne, L.; Bai, Y. W.; Englander, S. W. *J. Am. Chem. Soc.* **1994**, *116*, 6482.
(59) Schmitt, M. A.; Choi, S. H.; Guzei, I. A.; Gellman, S. H. *J. Am. Chem. Soc.* **2006**, *128*, 4538.
(60) Hayen, A.; Schmitt, M. A.; Ngassa, F. N.; Thomasson, K. A.; Gellman, S. H. *Angew. Chem., Int. Ed. Engl.* **2004**, *43*, 505.
(61) Connelly, G. P.; Bai, Y.; Jeng, M. F.; Englander, S. W. *Proteins: Struct., Funct., Genet.* **1993**, *17*, 87.
(62) Bai, Y.; Milne, J. S.; Mayne, L.; Englander, S. W. *Proteins: Struct., Funct., Genet.* **1993**, *17*, 75.
(63) Bai, Y.; Englander, J. J.; Mayne, L.; Milne, J. S.; Englander, S. W. *Methods Enzymol.* **1995**, *259*, 344.
(64) Mohamadi, F.; Richards, N. G. J.; Guida, W. C.; Liskamp, R.; Lipton, M.; Caufield, C.; Chang, G.; Hendrickson, T.; Still, W. C. *J. Comput. Chem.* **1990**, *11*, 440.
(65) *Macromodel*, version 9.9, Schrodinger, Inc.: New York, 2011.
(66) Murray, J. K.; Gellman, S. H. *Biopolymers* **2007**, *88*, 657.
(67) Murray, J. K.; Farooqi, B.; Sadowsky, J. D.; Scalf, M.; Freund, W. A.; Smith, L. M.; Chen, J. D.; Gellman, S. H. *J. Am. Chem. Soc.* **2005**, *127*, 13271.
(68) Knight, S. M.; Umezawa, N.; Lee, H. S.; Gellman, S. H.; Kay, B. K. *Anal. Biochem.* **2002**, *300*, 230.
(69) Harker, E. A.; Daniels, D. S.; Guarracino, D. A.; Schepartz, A. *Bioorg. Med. Chem.* **2009**, *17*, 2038.
(70) Kritzer, J. A.; Lear, J. D.; Hodsdon, M. E.; Schepartz, A. *J. Am. Chem. Soc.* **2004**, *126*, 9468.
(71) Harker, E. A.; Schepartz, A. *ChemBioChem* **2009**, *10*, 990.
(72) Vazquez, A.; Bond, E. E.; Levine, A. J.; Bond, G. L. *Nat. Rev. Drug Discovery* **2008**, *7*, 979.
(73) Seebach, D.; Abele, S.; Gademann, K.; Guichard, G.; Hintermann, T.; Jaun, B.; Matthews, J. L.; Schreiber, J. V.; Oberer, L.; Hommel, U.; Widmer, H. *Helv. Chim. Acta* **1998**, *81*, 932.
(74) Kapitán, J.; Zhu, F.; Hecht, L.; Gardiner, J.; Seebach, D.; Barron, L. D. *Angew. Chem., Int. Ed.* **2008**, *47*, 6392.
(75) Daniels, D. S.; Petersson, E. J.; Qiu, J. X.; Schepartz, A. *J. Am. Chem. Soc.* **2007**, *129*, 1532.
(76) Horne, W. S.; Price, J. L.; Gellman, S. H. *Proc. Natl. Acad. Sci. U.S.A.* **2008**, *105*, 9151.
(77) Karplus, M. *J. Chem. Phys.* **1959**, *30*, 11.
(78) Pardi, A.; Billeter, M.; Wuthrich, K. *J. Mol. Biol.* **1984**, *180*, 741.
(79) Roehrl, M. H.; Wang, J. Y.; Wagner, G. *Biochemistry* **2004**, *43*, 16056.